Atmospheric Blocking Pattern Recognition in Global Climate Model Simulation Data

Grzegorz Muszynski[1,2], **Prabhat**[2], **Jan Balewski**[2], **Karthik Kashinath**[2], **Michael Wehner**[3], **Vitaliy Kurlin**[1]

1) Computer Science Department, University of Liverpool, United Kingdom
2) NERSC, Lawrence Berkeley National Laboratory, United States
3) CRD, Lawrence Berkeley National Laboratory, United States

muszyng@liverpool.ac.uk

Introduction & Scientific Motivation

- We address a problem of Atmospheric Blocking (AB) pattern recognition in global climate datasets, such as climate reanalyses and climate model simulations.
- ABs are large-scale climate patterns (see Fig. 1) that have the following features:
  - They are persistent obstructions of the normal west-to-east air circulation pattern.
  - They are stationary events that persist for several days or even weeks over certain region.
  - They are often associated with extreme weather events (e.g. severe heat waves, cold spells, and floods).

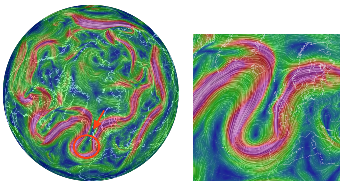

Figure 1: Left: an example of Atmospheric Blocking (AB) pattern over the Atlantic European coast. Right: a close-up of the AB pattern. Shown is the wind speed field ($m\ s^{-1}$). Source: the US NWS data visualised by http://earth.nullschool.net.

- The main objectives are the classification and localisation of ABs in mid-latitude regions (see Fig. 2). Because ABs are often correlated with extreme weather events, including the severe heat waves or cold snaps in Europe, North America, and other parts of the globe.

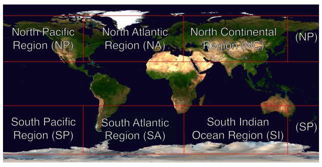

Figure 2: An example of the world map (globe) with six regions used in this study: the North Pacific Region (NP); the North Atlantic Region (NA); the North Continental Region (NC); the South Pacific Region (SP); the South Atlantic Region (SA), and the South Indian Ocean Region (SI).

Materials and Methodology

Dataset

- Data in this study are the ERA-Interim reanalysis from the European Center for Medium-Range Weather Forecasting, and binary masks (i.e., AB or non-AB labels) have been provided by the Institute for Atmospheric and Climate Science at the ETH Zurich, Switzerland (see Fig. 3, "Input").
- We use temperature, meridional and zonal winds, geopotential height, and potential vorticity variables at 8 pressure levels, 6-hourly at approx. 80 km spatial resolution in the period of 1979-2018.
- Each geographic region in Figure 2 is roughly centered over a local maximum of AB frequency and has a size of 60 pixels $\times$ 120 pixels $\times$ 40 channels.
- The location of ABs is described by the centroid or the mass centre of binary blobs in each region and radius of minimum circular bounding boxes.

Methodology

We propose a AB pattern recognition method that consists of two stages, as shown in Figure 3:

- In the first stage, a convolutional neural network (CNN) based classifier distinguishes the AB images from the non-AB images in different regions over the globe. Those images with detected AB events are passed to the second stage.
- Next, a CNN-based regressor predicts AB location parameters in the images, i.e. a mass centre (a latitudinal position and a longitudinal position), and a radius of a minimum enclosing circular box of these events in different regions of the globe.

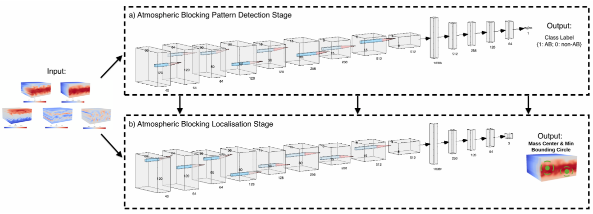

Figure 3: The scheme of a hierarchical atmospheric blocking pattern recognition method.

- A hierarchical structure of classification and localisation method consists of two layers: i) classification layer of ABs using CNN models (binary classification); ii) localisation layer of AB using CNN models (regression).
- Both stages (layers) employ customised CNN architectures inspired by the Visual Geometry Group (VGG) architectures. The architectures vary in the depth (i.e., the number of convolutional layers), the number of filters, and the number of fully connected layers and neurons, as shown in Table 1.

CNN Architectures				
A	B	C	D	E
Input: ($60 \times 120 \times 40$)				
conv-64	conv-64	conv-64	conv-64	conv-64
	conv-64	conv-64	conv-64	conv-64
Maxpooling				
conv-128	conv-128	conv-128	conv-128	conv-128
		conv-128	conv-128	conv-128
Maxpooling				
conv-256	conv-256	conv-256	conv-256	conv-256
			conv-256	conv-256
Maxpooling				
conv-512	conv-512	conv-512	conv-512	conv-512
				conv-512
Maxpooling				
FC-512 or —				
FC-256 or FC-256				
FC-128 or FC-128				
FC-64 or FC-64				
Output: FC-1 or FC-3				

Table 1: Convolutional neural network (CNN) architectures are shown in columns. The depth of the architectures increases from the left (A) to the right (E). The parameters of both types of layers are denoted as follows: conv-(number of filters); FC-(number of channels).

Results

To assess the performance of architectures of the CNN-based classifier and regressor, we use the following metrics: a classification accuracy (ACC) and F1 score for the classification task; Lin's concordance correlation coefficient (CCC) and the mean percentage error (MPE) for the localisation task. Here, we present the classification and regression results in Fig. 4 and Fig. 5, respectively.

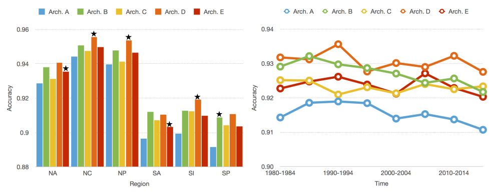

Figure 4: Performance of CNN architectures: architecture A, architecture B, architecture C, architecture D, and architecture E; for regions shown in Fig. 2. Left bar chart illustrates classification accuracy for each architecture per region and the right chart illustrates the mean classification accuracy of each architecture per region over five year periods. The $\star$ symbol stands for a p-value $\ll 0.05$.

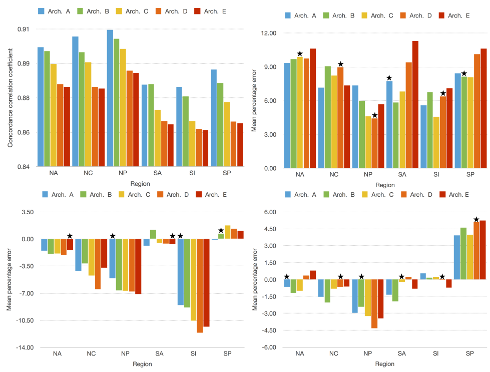

Figure 5: Performance of CNN architectures: architecture A, architecture B, architecture C, architecture D, and architecture E; for regions shown in Fig. 2. Top left bar chart illustrates the Lin's concordance correlation coefficient for each architecture per region. The top right chart displays illustrates mean percentage error for each architecture in estimating the latitudinal position of the mass centre of atmospheric blocks (ABs) per region. The bottom left chart shows shows mean percentage error for each architecture in estimating the longitudinal position of the mass centre of ABs per region. The bottom right chart illustrates mean percentage error for each architecture in estimating the radius of the mass centre of ABs per region. The $\star$ symbol stands for a p-value $\ll 0.05$.

Conclusion and Future Work

- We propose the AB pattern recognition method that consists of two stages: AB classification and localisation. We explore five CNN architectures and evaluate their performance in six geographical regions over the globe.
- The results indicate that the AB classification performance significantly increases for the deep CNN architectures. In contrast, we see the estimation error of event location significantly decreases in the localisation problem for the shallow CNN architectures.
- We demonstrate that CNN architectures achieve higher accuracy for AB classification and lower estimation error of AB localisation in regions of the Northern Hemisphere than in regions of the Southern Hemisphere.